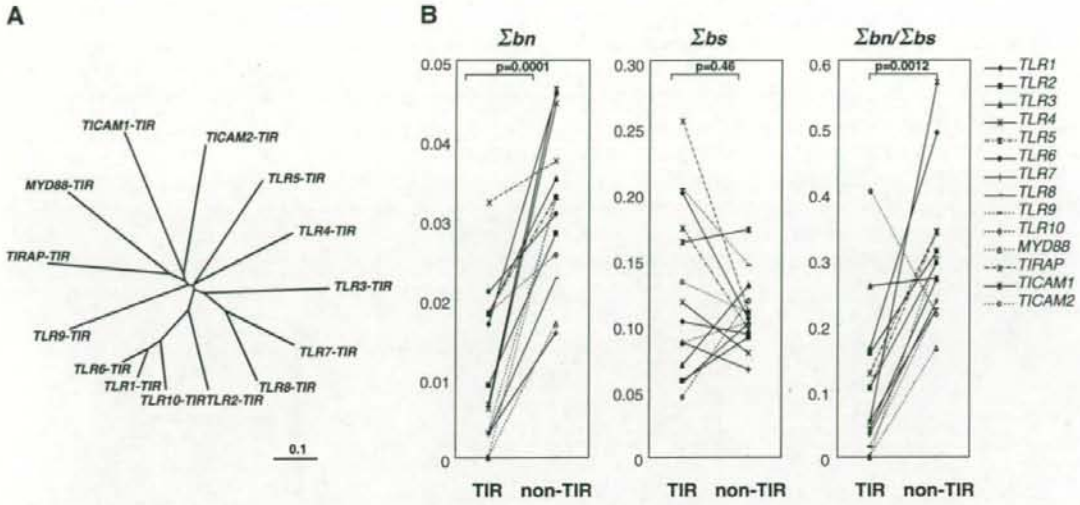

Fig. 2 **a** A neighbor-joining phylogenetic tree for 14 human sequences encoding TIR domains. Alignment and neighbor-joining tree for sequences was inferred using the Clustal X (Thompson et al. 1997) and TreeView programs. **b** The values of Σbn, Σbs, and Σbn/Σbs for the TIR domains and non-TIR coding regions of 14 genes, including *TLRs* (*TLR1–10*), *MYD88*, *TILAP*, *TICAM1*, and *TICAM2*. Statistical significance was tested with the Wilcoxon matched-pairs signed-ranks test

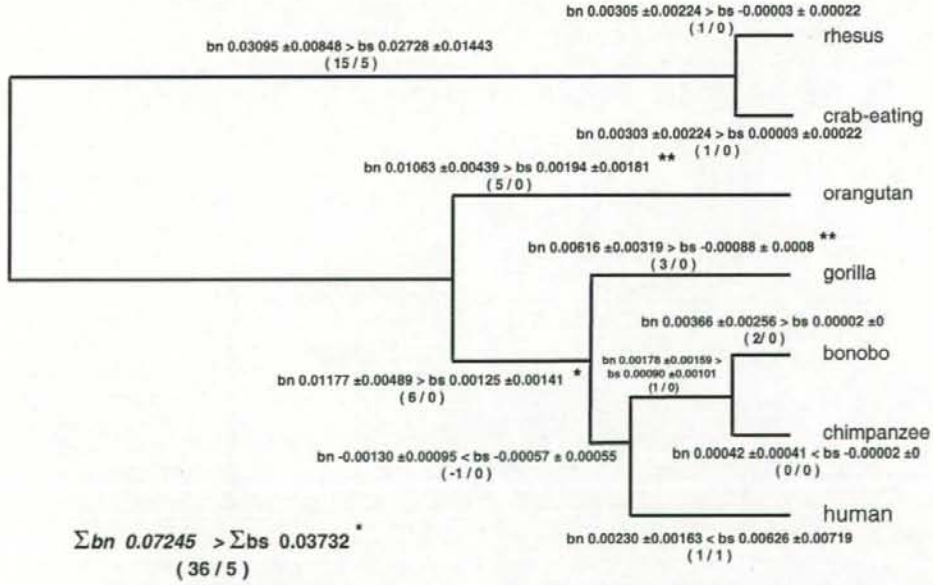

Fig. 3 Phylogenetic tree and the value of bn and bs for the selection target in the extracellular domain of TLR4 among seven primate species. We applied the Bn–Bs program (Zhang et al. 1998) to evaluate the value of bn and bs in individual branches of the primate phylogenetic tree (the values were shown with standard errors). Numbers of non-synonymous/synonymous substitutions for each branch are shown in *parentheses*. The values of bn in three lineages since the emergence of great apes were significantly higher than those of bs (*$p<0.05$ and **$p<0.01$ in Z test)

The estimated values of bn are larger than those of bs in several lineages among hominoids and Old World monkey, which is much evident in the lineages among hominoids. These lineages have a relatively low value of bs. On the other hand, the most estimated value of bn in the lineages among New World monkeys and prosimians are lower than those of bs (Fig. 3a, Supplementary material, Table S2; Fig. 4). Similar findings were shown in the analyses of synonymous (Ks) and non-synonymous nucleotide substitution rate (Ka) for the pairing of the 21 primate sequences at the target region of *TLR4* are shown in Fig. 3b and Supplementary material, Table S1. The Ka/Ks ratios from the comparisons among hominoids and Old World monkeys were much higher than 1.0; however, all values from the comparisons among New World monkeys and prosimians were under 1.0.

Ancestral amino acid sequence for 21 primates was estimated by a parsimony method using PROTPARS program in PHYLIP (Felsenstein 1989; Fig. 5). Among 210 amino acids from TLR4 target region, less than 50% of

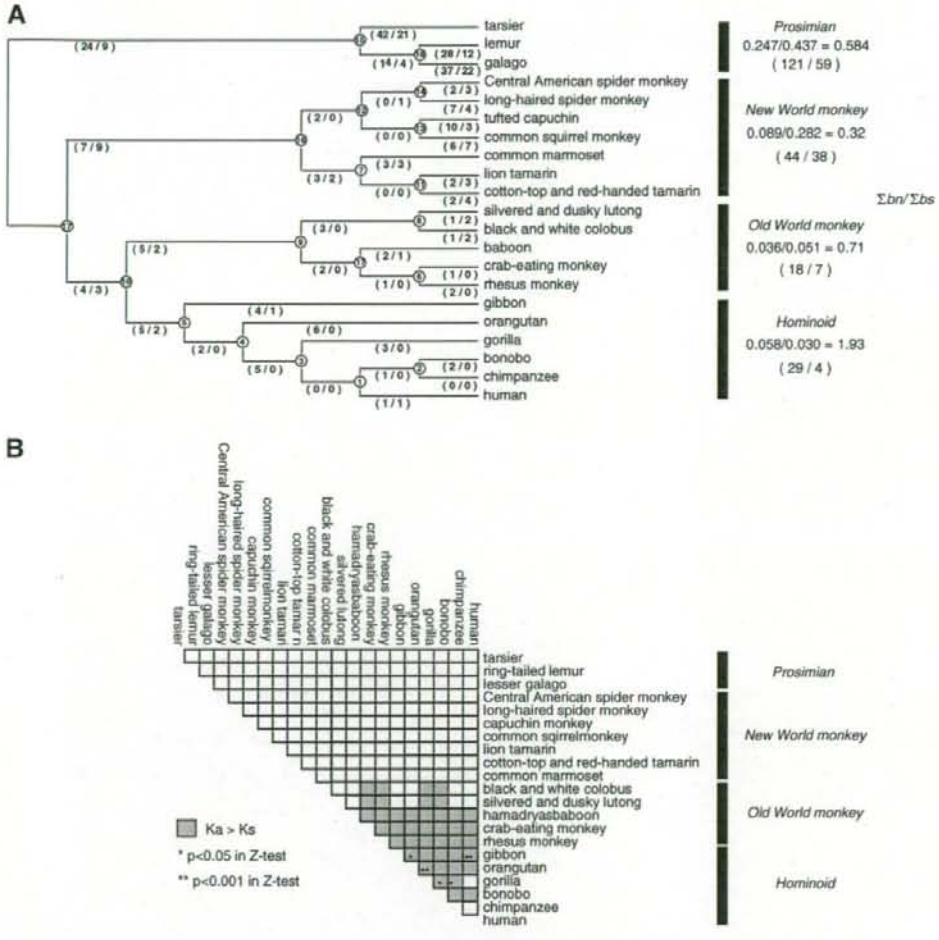

Fig. 4 **a** Phylogenetic tree and the nucleotide substitutions for the extracellular domain of TLR4 from 21 sequences. We applied the Bn–Bs program (Zhang et al. 1998) to evaluate the values of bn and bs in individual branches of the primate phylogenetic tree. *Numbers in parentheses* indicate the number of nucleotide substitutions at non-synonymous/synonymous sites. In several lineages, the value of bn is larger than that of bs (Table S3). Σbn and Σbs indicate the value summing up bn and bs, respectively, in the lineages from hominoids, Old World monkeys, and New World monkeys. Branches are not scaled. *Numbered circles* are used to specify individual branches and are referenced in Supplementary material, Table S3. **b** Ka/Ks ratios for all comparisons among 21 TLR4 target sequences. The values of Ka/Ks for 627-bp target sequences were evaluated, because the comparisons among 21 sequences showed that a 3-bp deletion were observed in sequences from lesser galago (*G. senegalensis*) and ring-tailed lemur (*L. catta*)

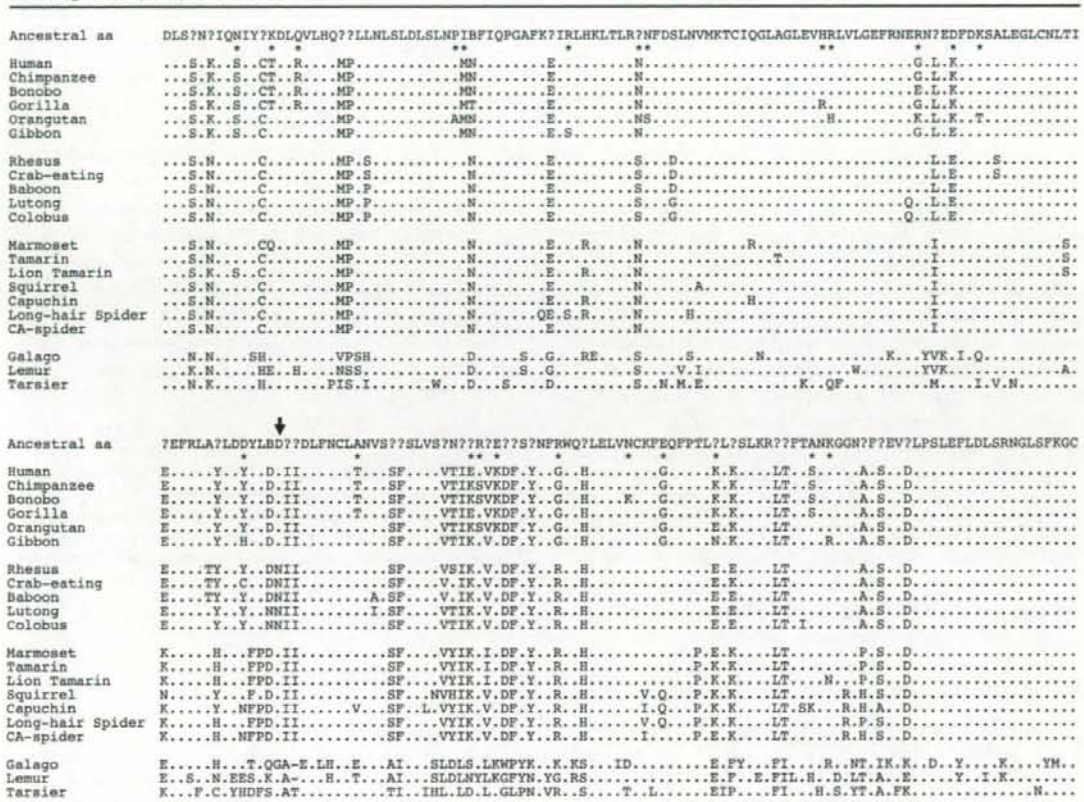

Fig. 5 Alignment of TLR4 target amino acid sequences of 21 primate species. *Dots* indicate identity to the ancestral sequence predicted by PROTPARS program in PHYLIP (Tamura et al. 2007), and *dashes* indicate a gap. *Asterisks* indicate amino acids which had been substituted since the emergence of hominoids. *Arrow* indicates the position corresponding to human mutation, D299G. The protein sequences are given by the *one-letter code* and consistent with the IUB standard abbreviations. *Question marks* in the ancestral amino acid sequence indicate the amino acid of which ancestral sequence was not determined by PROTPARS program (Felsenstein 1989)

amino acids [42.9% (90/210)] were conserved among 21 primate species, and at least 24 amino acids were replaced since the emergence of hominoids.

Discussion

Several lines of evidence suggested that genes linked to immune and defense systems are good candidate genes under the pressure of positive natural selection. However, most of the TLR-related genes have come under negative natural selection in the course of primate evolution. Our study suggested that the genomic segments encoding the intracellular TIR domains have undergone strong purifying selection and that the extracellular domain of TLR4 has been a single target of positive Darwinian selection among the TLR-related genes. We have no strong evidence that the extracellular domains of other TLRs, which recognize a variety of pathogen-associated molecules, has been under the pressure of natural selection in the course of primate evolution.

The TIR domains are key components in TLR signal transduction. In particular, an adaptor protein, MYD88, is tightly linked to all of the TLR signaling pathways except for TLR3 (Akira et al. 2006; Bowie and O'Neill 2000). This may be the reason for that the amino acid sequences have not been altered in the course of primate evolution. Most of mutations arising at the TIR domains would in all likelihood have been deleterious and thus reduced the fitness in the primates who harbored such changes.

Among the TLRs, *TLR7*, *TLR8*, and *TLR9* have much lower values of Σbn at the TIR domains. These three genes recognize nucleic acids in the innate immune system and are categorized into highly related subfamilies based on phylogenetic comparison (Akira et al. 2006). TLR7 and TLR8 are known to recognize single-strand RNA molecules

and the natural ligand of TLR9 is CpG motif-containing DNA (Akira et al. 2006; Heil et al. 2004). *TLR7* and *TLR8* are also mapped on chromosome X in the human, chimpanzee, and rhesus macaque genome, which might be linked to the reduced Σbn for these two genes in primate evolution, because reduced divergence has been observed in chromosome X when a comparison was performed on the human and rhesus macaque genome (Rhesus Macaque Genome Sequencing and Analysis Consortium 2007).

On the other hand, it is likely that the part of the extracellular domain of TLR4 has been under the pressure of positive natural selection in the several lineages since the emergence of Catarrhina. The values of bn were higher than those of bs in the several lineages. In particular, the values of bn in the lineages of gorilla and the lineage just after the split of ancestors of four great apes (gorilla, bonobo, chimpanzee, and human) were much larger than the estimated value of bs for entire TLR4 coding sequences. However, we cannot rule out the possibility that chance variation in the value of bs, rather than positive selection, accounted for the observed pattern (Hughes and Friedman 2008), because these lineages have a relatively low value of bs.

This suggestive *TLR4* target region, which encodes the extracellular domain next to the domain with LRR, has been reported to be hypervariable and to contribute to species-specific recognition of several molecules such as taxol, a lipid IVa, and LPS (Smirnova et al. 2000; Hajjar et al. 2002; Lien et al. 2000). Our study showed that the positions of amino acid replacements since the emergence of Catarrhina, which might be linked to species-specific recognition of LPS, are widely distributed in the TLR4 selection target. This target region also has been reported to be linked to the susceptibility to LPS in humans (Arbour et al. 2000). A missense human mutation D299G, in which an aspartic acid is replaced by a glycine at the 299 amino acid position of human TLR4, is associated with a blunted response to LPS and increased susceptibility to Gram-negative bacterial infections. An aspartic acid at the 299 amino acid position of human TLR4 is highly conserved among great apes and gibbon, whereas an aspartic acid has been replaced by a glycine in the lineage of Old World Monkeys (Fig. 5). These results indicated that the sensitivity to a certain type of LPS might differ between great apes and Old World Monkeys.

Given that TLR4 recognizes a wide variety of ligands such as LPS and viral envelope proteins, the differences in the species-specific susceptibility to infectious disease might have been linked to natural selection pressure. It is widely accepted that the susceptibility to infectious pathogens differ among primates. For example, Asian Old World monkeys are highly susceptible to infection with *M. tuberculosis* bacilli, while New World monkeys appear to be fairly resistant (Isaza 2003). Furthermore, the species-specific restrictions operating on HIV-1 infection are well known. Humans as well as chimpanzees but not New and Old World monkeys are susceptible to HIV-1 (Stremlau et al. 2004). Though we are not aware of the exact pathogens, it is highly possible that wide-spread pathogens might have been linked to the selective pressure for TLR4.

In this study, we evaluated the molecular evolution of TLR-related genes in primates and concluded that natural selection has indeed shaped the sequence patterns of TLR-related genes in the course of primate evolution, but positive selection pressure has been limited across the TLR family.

Acknowledgments This work was supported in part by Grant-in-Aid for Scientific Research from the Ministry of Education, Culture, Sports, Science and Technology, Japan and research grants from the Ministry of Health, Labor and Welfare, Japan, the Japan Health Science Foundation, and the program of Founding Research Centers for Emerging and Reemerging Infection Disease supported by the Ministry of Education, Culture, Sports, Science, and Technology, Japan.

References

Akira S, Uematsu S, Takeuchi O (2006) Pathogen recognition and innate immunity. Cell 124:783–801

Arbour NC, Lorenz E, Schutte BC, Zabner J, Kline JN, Jones M, Frees K, Watt JL, Schwartz DA (2000) TLR4 mutations are associated with endotoxin hyporesponsiveness in humans. Nat Genet 25:187–191

Bennetzen JL, Hall BD (1982) Codon selection in yeast. J Biol Chem 257:3026–3031

Bowie A, O'Neill LA (2000) The interleukin-1 receptor/Toll-like receptor superfamily: signal generators for pro-inflammatory interleukins and microbial products. J Leukoc Biol 67:508–514

Felsenstein J (1989) PHYLIP—Phylogeny Inference Package (Version 3.2). Cladistics 5:164–166

Hajjar AM, Ernst RK, Tsai JH, Wilson CB, Miller SI (2002) Human Toll-like receptor 4 recognizes host-specific LPS modifications. Nat Immunol 3:354–359

Heil F, Hemmi H, Hochrein H, Ampenberger F, Kirschning C, Akira S, Lipford G, Wagner H, Bauer S (2004) Species-specific recognition of single-stranded RNA via Toll-like receptor 7 and 8. Science 303:1526–1529

Hughes AL, Friedman R (2008) Codon-based tests of positive selection, branch lengths, and the evolution of mammalian immune system genes. Immunogenetics 60:495–506

Isaza R (2003) Tuberculosis in all taxa. In: Fowler ME, Miller RE (eds) Zoo and wild animal medicine, 5th edn. Elsevier, St. Louis, pp 689–696

Lien E, Means TK, Heine H, Yoshimura A, Kusumoto S, Fukase K, Fenton MJ, Oikawa M, Qureshi N, Monks B, Finberg RW, Ingalls RR, Golenbock DT (2000) Toll-like receptor 4 imparts ligand-specific recognition of bacterial lipopolysaccharide. J Clin Invest 105:497–504

Marchler-Bauer A, Bryant SH (2004) CD-Search: protein domain annotations on the fly. Nucleic Acids Res 32(W):327–331

Nagai Y, Akashi S, Nagafuku M, Ogata M, Iwakura Y, Akira S, Kitamura T, Kosugi A, Kimoto M, Miyake K (2002) Essential

role of MD-2 in LPS responsiveness and TLR4 distribution. Nat Immunol 3:667–672

Nei M, Gojobori T (1986) Simple methods for estimating the numbers of synonymous and nonsynonymous nucleotide substitutions. Mol Biol Evol 3:418–426

Poltorak A, He X, Smirnova I, Liu MY, Van Huffel C, Du X, Birdwell D, Alejos E, Silva M, Galanos C, Freudenberg M, Ricciardi-Castagnoli P, Layton B, Beutler B (1998) Defective LPS signaling in C3H/HeJ and C57BL/10ScCr mice: mutations in Tlr4 gene. Science 282:2085–2088

Rhesus Macaque Genome Sequencing and Analysis Consortium, Gibbs RA, Rogers J, Katze MG, Bumgarner R, Weinstock GM, Mardis ER, Remington KA, Strausberg RL, Venter JC, Wilson RK, Batzer MA, Bustamante CD, Eichler EE, Hahn MW, Hardison RC, Makova KD, Miller W, Milosavljevic A, Palermo RE, Siepel A et al (2007) Evolutionary and biomedical insights from the rhesus macaque genome. Science 316:222–234

Rozas J, Sanchez-DelBarrio JC, Messeguer X, Rozas R (2003) DnaSP, DNA polymorphism analyses by the coalescent and other methods. Bioinformatics 19:2496–2497

Shimazu R, Akashi S, Ogata H, Nagai Y, Fukudome K, Miyake K, Kimoto M (1999) MD-2, a molecule that confers lipopolysaccharide responsiveness on Toll-like receptor 4. J Exp Med 189:1777–1782

Smirnova I, Poltorak A, Chan EK, McBride C, Beutler B (2000) Phylogenetic variation and polymorphism at the toll-like receptor 4 locus (TLR4). Genome Biol 1:research002.1–002.10

Smirnova I, Hamblin MT, McBride C, Beutler B, Rienzo AD (2001) Excess of rare amino acid polymorphisms in the Toll-like Receptor 4 in humans. Genetics 158:1657–1664

Stremlau M, Owens CW, Perron MJ, Kiessling M, Autissier P, Sodroski J (2004) The cytoplasmic body component TRIM5-alpha restricts HIV-1 infection in Old World monkeys. Nature 427:848–853

Tamura K, Dudley J, Nei M, Kumar S (2007) MEGA4: Molecular Evolutionary Genetics Analysis (MEGA) Software Version 4.0. Mol Biol Evol 24:1596–1599

Thompson JD, Gibson TJ, Plewniak F, Jeanmougin F, Higgins DG (1997) The CLUSTAL_X windows interface: flexible strategies for multiple sequence alignment aided by quality analysis tools. Nucleic Acids Res 25:4876–4882

Wellcome Trust Case Control Consortium (2007) Genome-wide association study of 14,000 cases of seven common diseases and 3,000 shared controls. Nature 447:661–678

Zhang J, Rosenberg HF, Nei M (1998) Positive Darwinian selection after gene duplication in primate ribonuclease genes. Proc Natl Acad Sci USA 95:3708–3713

Gene 432 (2009) 60–66

Contents lists available at ScienceDirect

Gene

journal homepage: www.elsevier.com/locate/gene

Molecular cloning and characterization of the common marmoset huntingtin gene

Hirohiko Hohjoh [a,*], Hirofumi Akari [b], Yuko Fujiwara [a,c], Yoshiko Tamura [a], Hirohisa Hirai [d], Keiji Wada [c]

[a] Department of Molecular Genetics, National Institute of Neuroscience, NCNP, 4-1-1 Ogawahigashi, Kodaira, Tokyo 187-8502, Japan
[b] Laboratory of Disease Control, Tsukuba Primate Research Center, National Institute of Biomedical Innovation, Tsukuba, Ibaraki, Japan
[c] Department of Degenerative Neurological Diseases, National Institute of Neuroscience, NCNP, Kodaira, Tokyo, Japan
[d] Primate Research Institute, Kyoto University, Inuyama, Aichi, Japan

ARTICLE INFO

Article history:
Received 24 July 2008
Received in revised form 4 November 2008
Accepted 5 November 2008
Available online 24 November 2008

Received by M. Di Giulio

Keywords:
Common marmoset
Huntingtin
Gene silencing
Immortalized cell line

ABSTRACT

We report here for the first time the isolation and identification of the common marmoset (*Callithrix jacchus*) *huntingtin* (*Htt*) gene, whose ortholog in humans is known to be related to Huntington's disease (HD). A 9396 nucleotide complementary DNA (cDNA) carrying the putative full-length open reading frame of the marmoset *Htt* gene was identified, and highly conserved nucleotide and amino acid sequences among primates were observed. Based on this data and using tools evaluated for the detection of the marmoset *Htt* gene, we have demonstrated gene silencing against the expression of endogenous *Htt* gene in immortalized common marmoset mononuclear cells by means of RNA interference (RNAi). Taken together, the data presented here may assist us in realizing a non-human primate HD model with the common marmoset.

1. Introduction

Huntington's disease (HD) is an autosomal dominant neurodegenerative disease characterized by progressive and selective neural cell death associated with choreic movement and dementia (Walker, 2007). The responsible gene for HD, the huntingtin (Htt) gene, has been identified on chromosome 4q16.3 (Gusella et al., 1983; Gilliam et al., 1987), and an aberrant length of a CAG triplet repeat in exon 1, followed by expanded tracts of polyglutamine in the Htt polypeptide, is greatly involved in the onset of HD (Huntington's-Disease, 1993). Although the molecular mechanisms of either normal or aberrant Htt protein are still poorly understood, HD model animals (Mangiarini et al., 1996; Kazemi-Esfarjani and Benzer, 2000; von Horsten et al., 2003) and cells (Lunkes and Mandel, 1998) for understanding the pathogenesis of HD and developing therapies have been established by means of genetic engineering based on the genetic information of *Htt*. The use of an animal model that is closely related to humans may be particularly promising.

The common marmoset (*Callithrix jacchus*) is classified into the Callitrichidae family of Platyrrini (New World monkeys) and has been used as a non-human primate experimental animal in various research fields including gene therapy, autoimmune disease, organ transplantation, and pharmacology (Kendall et al., 1998; Doods et al., 2000; Deisboeck et al., 2003; t'Hart et al., 2003). Accordingly, it is worth promoting studies with the common marmoset aimed at overcoming neurodegenerative diseases such as HD, as the animal's close relationship to humans makes it well suited to this kind of study. Indeed, a recent study has generated a non-human primate HD model with the rhesus monkey (*Macaca mulatta*) (Palfi et al., 2007; Yang et al., 2008).

In this report, we describe for the first time the isolation and characterization of a cDNA encoding the putative full-length open reading frame of the common marmoset *Htt* gene, and present experimental data based on the isolated cDNA. The data presented here may provide us with useful information for establishing non-human primate HD models with the common marmoset.

2. Materials and methods

2.1. Preparation of total RNA

Common marmoset total RNA was isolated from the brain tissue of a stillborn marmoset fetus and immortalized monocytes (described below) using Trizol (Invitrogen). The experiments with the common marmoset complied with protocols approved by the ethical committee for primate research of the National Center of Neurology and Psychiatry and adhered to the legal requirements of Japan.

Abbreviations: HD, Huntington's disease; Htt, huntingtn; RNAi, RNA interference; cDNA, complementary DNA; PBMC, peripheral blood mononuclear cell; RT, reverse transcription; PCR, polymerase chain reaction; ORF, open reading frame; APP, amyloid precursor protein; GAPDH, glyceraldehyde-3-phosphate dehydrogenase; GFP, green fluorescence protein; CMV, Cytomegalovirus.

* Corresponding author.
E-mail address: hohjohh@ncnp.go.jp (H. Hohjoh).

0378-1119/$ – see front matter © 2008 Elsevier B.V. All rights reserved.
doi:10.1016/j.gene.2008.11.012

2.2. Established common marmoset cell lines

Adult common marmosets being reared at the Primate Research Institute of Kyoto University or Tsukuba Primate Research Center were anesthetized by ketamine, which was approved by the Animal Welfare and Animal Care Committees of both institutes, and peripheral blood was collected. From the collected blood samples, peripheral blood mononuclear cells (PBMCs) were purified and immortalized by infection of a 488-77 strain of *Herpesvirus saimiri* (kindly provided by Dr. R. C. Desrosiers) as previously described (Akari et al., 1996). The established marmoset cell lines, designated HSCj-110, HSCj-009, and HSCj-002, were phenotypically activated CD3+T lymphocytic cells and grown in RPMI-1640 medium (Sigma) supplemented with 10% FCS, 50 mM 2-mercaptoethanol, and antibiotics.

2.3. Reverse transcription – (real time) polymerase chain reaction [RT-(real time) PCR]

The common marmoset total RNAs were subjected to complementary DNA (cDNA) synthesis using oligo(dT) primers and a Superscript III reverse transcriptase (Invitrogen), according to the manufacturer's instructions, and polymerase chain reaction (PCR) using the cDNAs as templates was carried out by means of the ABI GeneAmp PCR system 9700 (Applied Biosystems). In the case of real time PCR, the cDNAs were examined by the AB 7300 Real Time PCR System (Applied Biosystems) with a TaqMan Universal PCR Master Mix together with Assays-on-Demand Gene Expression products (Applied Biosystems) or a SYBR Green PCR Master Mix together with Perfect Real Time Primers (Takara Bio) or designed PCR primers, according to the manufacturers' instructions. Synthesized oligonucleotide primers and purchased primer and probe were as follows:

Synthesized oligonucleotide primers:

HD1-F: 5′-TATAGAATTCGGGAGACCGCCATGGCGAC-3′
HD1-ORF-R: 5′-TCAAGCGGCCGCTCAGCAGGTGGTGACCTTG-3′
HD1-1900R2: 5′-TAAAGGATCCCCGTCTAACACAATTTCAG-3′
cjHtt(1139)-F: 5′-TTATAGCTGGAGGCGGTTCC-3′
cjHtt(1254)-R: 5′-GACGTCCGACCTCGATTCAG-3′

Purchased primer and probe:

Assays-on-Demand Gene Expression product for the human *Htt* gene (Assay ID: Hs00169273_m1) (Applied Biosystems).

Perfect Real Time Primers for the human *GAPDH* gene (Primer-Set ID: HA067812) (Takara Bio).

2.4. Cloning and sequence analysis of the full-length ORF of the marmoset Htt gene

Complementary DNA derived from the common marmoset total RNA was subjected to PCR amplification using *TaKaRa LA Taq* polymerase (TAKARA BIO) with the HD1-F and HD1-ORF-R primers under the following thermal cycling conditions: heat denaturation at 94 °C for 1 min, 30 cycles of amplification including denaturation at 94 °C for 20 s and extension at 68 °C for 12 min, and a final extension at 72 °C for 10 min. The PCR product was examined by agarose gel electrophoresis followed by ethidium bromide staining, and an approximately 9.4 kb PCR band (Fig. 1) was purified from the gels using a TOPO XL gel purification kit (Invitrogen). The resultant PCR product was inserted into the pCR-XL-TOPO plasmid with a TOPO XL PCR cloning kit (Invitrogen) and then sequence determination of the insert was carried out. To clarify uncertain nucleotide sequences, additional RT-PCR targeting of uncertain regions followed by sequence determination was performed and the precise nucleotide sequence was confirmed. The determined nucleotide sequence encoding a putative full-length ORF of the common marmoset *Htt* gene has been registered in the GenBank database: accession number, AB443866.

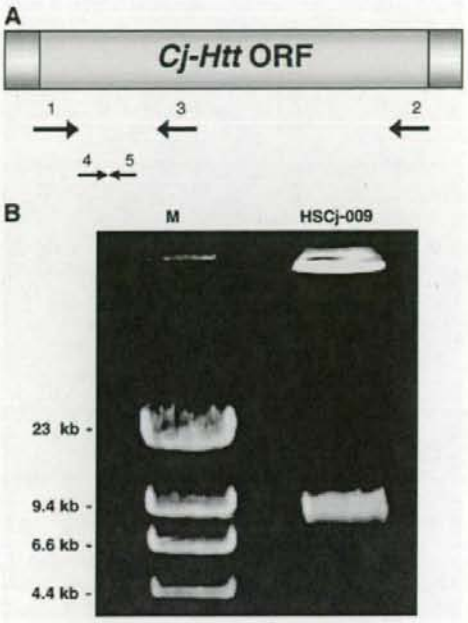

Fig. 1. RT-PCR amplification. (A) Schematic drawing of putative *Htt* cDNA. Open reading frame (ORF) is indicated by a yellow box. Arrows indicate synthesized PCR primers, which are designed in possibly conserved nucleotide sequences: 1, HD1-F; 2, HD1-ORF-R; 3, HD1-1900R2; 4, cjHtt(1139)-F; 5, cjHtt(1254)-R (detailed in Materials and methods). (B) RT-PCR. The first strand cDNA was synthesized by RT using RNA isolated from immortalized common marmoset mononuclear cells (HSCj-009) as a template and oligo(dT) as a primer. The following PCR was carried out using HD1-F and HD1-ORF-R primers. The resultant PCR products were analyzed by gel electrophoresis with 0.6 % agarose gel followed by ethidium bromide staining. Hind III-digested λDNA was used as a DNA size marker (M).

2.5. Western blotting

Equal amounts (~35 μg) of protein extracts from the common marmoset and mouse brain tissues and established PBMC lines (described above) were separated by SDS-PAGE with 5% polyacrylamide gels and electrophoretically blotted onto PVDF membranes (Millipore). Membranes were blocked for 1 h in blocking solution [5% non-fat milk in TBST buffer (25 mM Tris-HCl, pH 7.4, 150 mM NaCl and 0.1% Tween-20)] and incubated with 1/1000 dilution of mouse anti-huntingtin protein monoclonal antibodies [MAB2166 and MAB2170 (Chemicon); ab7666 (Abcam)] followed by washing in TBST buffer and further incubation with sheep anti-mouse Ig, HRP-linked whole Ab (GE Healthcare). Antigen-antibody complexes were visualized using ECL plus Western Blotting Detection Reagent (GE Healthcare). After detection of signals, the membranes were subjected to antibody removal in Re-Blot Plus strong antibody stripping solution (Chemicon) followed by washing in TBST buffer, and then incubated with 1/1000 dilution of mouse anti-APP [MAB348 (Chemicon)] monoclonal antibody. Subsequent processes were the same as described above.

2.6. Gene silencing of marmoset Htt by RNA interference

To monitor gene silencing against the common marmoset *Htt* gene, we constructed a reporter plasmid carrying the 5′-terminal region of the marmoset *Htt* linked with the *GFP* reporter gene: the PCR product obtained from RT-PCR with the HD1-F and HD1-1900R2 primers was

Table 1
Sequence homologies (%) among various species' *Htt* genes

Homo sapiens	*Callithrix jacchus*	*Canis lupus familiaris*	*Bos taurus*	*Sus scrofa*	*Mus musculus*	*Rattus norvegicus*
Homo sapiens	**95.1** **97.0**	87.0 92.0	84.0 89.5	84.1 88.6	86.1 91.2	85.8 91.2
Canis lupus familiaris		86.6 91.4	84.0 88.4	83.9 87.9	85.6 90.8	85.1 90.9
Callithrix jacchus			84.5 89.4	84.4 89.7	84.0 89.2	83.8 89.3
Bos taurus				86.8 89.3	81.2 87.1	81.3 87.4
Sus scrofa					80.9 86.9	80.8 87.2
Mus musculus						95.9 97.6
Rattus norvegicus						

Figures in upper and lower stands represent nucleotide and amino acid sequence homologies, respectively, between two species.

trimmed with EcoRI and BamHI, and inserted into the pd2EGFP-N1 plasmid (Clontech) treated with the same restriction enzymes. The resultant reporter (5′*Cj-Htt-GFP*) plasmid and synthetic siRNA duplex targeting the marmoset *Htt* (cjHtt-1 siRNA duplex) were cotransfected into mouse neuroblastoma Neuro2a cells by Lipofectamine 2000 transfection reagent (Invitrogen) as described previously (Sakai and Hohjoh, 2006). Two days after transfection, the cells were examined by a fluorescent microscope. When the endogenous marmoset *Htt* gene was inhibited by RNAi, the cjHtt-1 siRNA duplex (0.4 nmol/transfection) was introduced into HSCj-009 cells (1×10^6 cells/transfection) by means of a Nucleofector system (Amaxa Biosystems) according to the manufacturer's instructions. Two days after transfection, total RNA and cell lysate were prepared from the cells and examined by RT-real time PCR and Western blotting, respectively.

The nucleotide sequences of synthesized cjHtt-1 siRNA were as follows:

Sense: 5′-GCCUUUGAGUCCCUCAAGUUU-3′
Antisense: 5′-ACUUGAGGGACUCAAAGGCUU-3′

2.7. Sequence data and computational analyses

The *Htt* sequnece data derived from various species were as follows [GenBank accession number]: human (*Homo sapiens*) [NM_002111]; chimp (*Pan troglodytes*) [XM_517080]; rhesus macaque (*Macaca mulatta*) [XM_001086119]; canine (*Canis lupus familiaris*) [XM_536221]; bovine (*Bos taurus*) [XM_866758]; wild boar (*Sus scrofa*) [NM_213964]; mouse (*Mus musculus*) [NM_010414]; rat (*Rattus norvegicus*) [XM_573634]; chicken (*Gallus gallus*) [XM_420822]. Although the rhesus macaque Htt sequence [XM_001086119] contains 20 undetermined nuclotides at positons 4932–4951 followed by 6 suspensive amino acid sequences, the sequence was used and examined together with the other sequneces in this study.

Sequence homology analysis of either nucleotide or amino acid sequences was carried out by means of the GENETYX software (Software Development Co., Ltd., Tokyo, Japan), where all the parameters were set at default. For identification of the HEAT repeats in the Cj-Htt protein sequences, the REP program (http://www.embl-heidelberg.de/~andrade/papers/rep/search.html) developed by Andrade et al. was used.

3. Results and discussion

3.1. Isolation and characterization of the common marmoset Htt gene

To isolate and identify the common marmoset *Htt* (*Cj-Htt*) gene and/or gene products, we focused on conserved regions in the *Htt* gene and isolate cDNA clone of the *Cj-Htt* transcript. Highly homologous regions (sequences) between the human and mouse *Htt* genes, whose corresponding regions in the *Cj-Htt* gene were also expected to remain conserved, were selected, and PCR primers were designed for such regions. We add that such conserved regions are also detectable by BLAST search with the human *Htt* as a query on the Trace archive of the Cj-database in NCBI. RT-PCR with the designed primers and total RNA extracted from common marmoset brain tissue and established cell lines was carried out, and an approximately 9.4 kb long PCR product, which was expected to contain the full-length open reading frame (ORF) of *Cj-Htt*, was obtained (Fig. 1). The PCR product was subjected to sequence determination and then compared with various species' *Htt* genes. From the results, it was clear that the PCR product, which is 9396 nucleotides in length, was derived from the common marmoset *Htt* gene which encodes a predicted 3131 amino acid long Cj-Htt polypeptide (the sequence accession number in GenBank is AB443866). Sequence homologies in the *Htt* gene among various species are indicated in Table 1. From the data, it appears that both the nucleotide and predicted amino acid sequences of the *Cj-Htt*

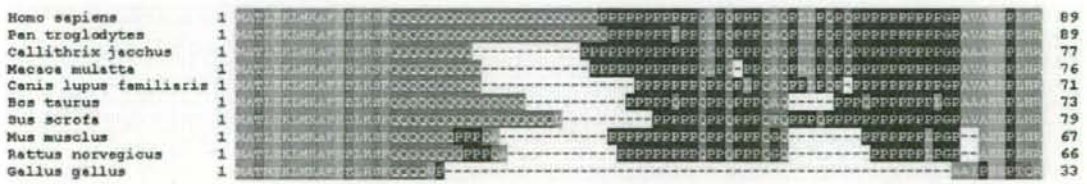

Fig. 2. Alignment of amino acid sequences in the Htt exon 1 and its corresponding regions. Sequence data were aligned based on the human Htt exon 1 (top line). Amino acid residues are color-coded based on the biochemical properties of the residues: hydrophobic amino acids in orange, polar amino acids with uncharged R groups in green, acidic amino acids in pink, basic amino acids in light blue, and special amino acids in dark blue.

Table 2
Alignment of HEAT repeats

Repeat*	Species**	AA position		Fragment†	Score	E-value
		From	To			
HEAT_AAA	Hs - Htt	124	162	QKLLGIAMELFLLCSDDAESDVRMVADECLNKVIKALMD	1510	1.26E-06
	Cj - Htt	112	150	QKLLGIAMELLLCSDDAESDVRMVADECLNKVIKALMD	1590	5.48E-07
HEAT_AAA	Hs - Htt	205	243	RPYLVNLLPCLTRTSKRPEESVQETLAAAVPKIMASPGN	1990	1.03E-04
	Cj - Htt	193	231	RPYLVNLLPCLTRTSKRPEESVQETLAAAVPKIMASPGN	1990	2.37E-08
HEAT_AAA	Hs - Htt	247	285	DNEIKVLLKAFIANLKSSSPTIRRTAAGSAVSICQHSRR	1590	5.48E-07
	Cj - Htt	235	273	DNEIKILLKAFIANLKSSSPTIRRTAAGSAVSICQHSRR	1590	1.97E-06
HEAT_AAA	Hs - Htt	317	355	LLTLRYLVPLLQQQVKDTSLKGSFGVTRKEMEVSPSAEQ	1620	1.11E-06
	Cj - Htt	305	343	LLTLRYLVPLLHQQVKDTSLKGSFGVTRKEMEVSPSAEQ	1570	1.46E-07
HEAT_ADB	Hs - Htt					
	Cj - Htt	734	771	YPEEQYVSDILNYIDHGDPQVRGATAILCGTLVCSILS	1450	3.29E-07
HEAT_AAA	Hs - Htt	803	841	TFSLADCIPLLRKTLKDESSVTCKLACTAVRNCVMSLCS	1500	5.78E-07
	Cj - Htt	791	829	TFSLADCVPLLRKTLKDESSVTCKLACTAVRHCVMSLCS	1449	2.90E-06
HEAT_AAA	Hs - Htt	904	942	KLQERVLNNVVIHLLGDEDPRVRHVAAASLIRLVPKLFY	1930	6.69E-08
	Cj - Htt	892	930	TLQERVLESVVIHLLGDEDPRVRHVAAASLIRLVPKLFY	2150	2.51E-05
HEAT_AAA	Hs - Htt	984	1025	RIYRGYNLLPSITDVTMENNLSRVIAAVSHELITSTTRALTF	1370	9.05E-06
	Cj - Htt	972	1013	RIYRGYNLLPSIIDVTMENNLSRVIAAVSHELITSTTRALTF	1410	2.71E-06
HEAT_AAA	Hs - Htt	1425	1463	RLFEPLVIKALKQYTTTTCVQLQKQVLDLLAQLVQLRVN	1370	5.62E-06
	Cj - Htt	1413	1451	RLFEPLVIKALKQYTTTTSVQLQKQVLDLLAQLVQLRVN	1580	3.20E-07
HEAT_AAA	Hs - Htt	2798	2836	DDTAKQLIPVISDYLLSNLKGIAHCVNIHSQQHVLVMCA	1430	3.51E-06
	Cj - Htt	2785	2823	DDTAKQLIPVISDYLLSSLKGLAHCVNTHSQQHVLVMCA	1430	3.29E-05

* HEAT_AAA and HEAT_ADB indicate subsets of HEAT repeats representing PP2A and adaptin families, respectively.
** Hs-Htt and Cj-Htt indicate the human and common marmoset Htt proteins, respectively.
†Amino acids which are different from the sequence of Hs-Htt are indicated in red.

cDNA have significant sequence homology to that of other species' *Htt* genes. In addition, it should be noted that *Htt* sequences between the human and common marmoset (colored in yellow in Table 1) appear to be particularly conserved as compared with sequence conservation within non-primate *Htt* genes, suggesting that the *Htt* gene is highly conserved in primates.

Fig. 2 shows the alignment of amino acid sequences encoded by *Htt* exon 1 and its corresponding region in various species. From the alignment, *Cj-Htt* appears to possess a short polyglutamine tract of nine glutamines compared with that of the human and chimpanzee *Htt* genes; but other than the polyglutamine tract, the exon 1 corresponding region in *Cj-Htt* exhibits high sequence homology to the human *Htt* exon 1. It is also interesting that polyproline region adjacent to the polyglutamine tract has differences between primates and non-primates: amino acid substitutions and deletions are observed, and the lack of the polyproline region in the *Gallus gallus Htt* exon 1 is particularly remarkable. These differences may influence folding and aggregation of the Htt protein, and might represent adaptive evolution of *Htt* to each species. The difference in the exon 1 among various species may provide us with a hint for understanding the expansion of the polyglutamine tract in Huntington's disease in human.

Other than the exon 1 region, we also investigated the HEAT repeats possessing tandem arrayed bihelical structure, which appear to wrap around target substrates (Andrade and Bork, 1995; Neuwald and Hirano, 2000), and found that the HEAT repeats are also conserved in the Cj-Htt protein (Table 2). In addition, it may be interesting that HEAT_ADB, a subset of HEAT repeats representing adaptin family, is present in Cj-Htt, but not in Hs-Htt.

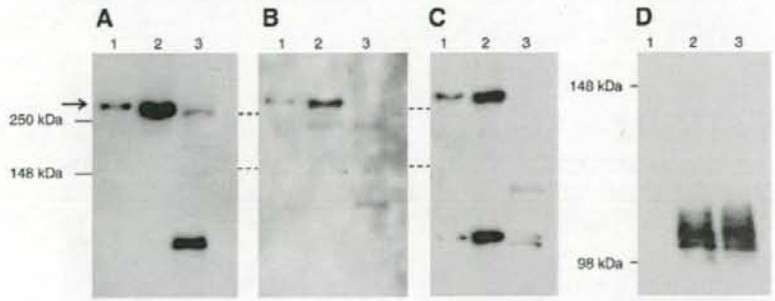

Fig. 3. Assessment of anti-human Htt antibodies against the common marmoset Htt polypeptide. Cell lysate derived from the common marmoset cell line (HSCj-110) (lane 1), brain tissue (lane 2), and mouse brain tissue as a control (lane 3) was examined by Western blotting with anti-human Htt antibodies. Tested antibodies were as follows: (A) MAB2166 (Chemicon), (B) MAB2170 (Chemicon), and (C) ab7666 (Abcam). Arrow indicates the signals of Htt proteins. The same results as those of HSCj-110 were also obtained when HSCj-002 and-009 were used (data not shown). After detection of signals, blotted membranes were subjected to antibody removal and then incubated with anti-APP antibody [MAB348 (Chemicon)] (D) followed by the same procedure as in the anti-human Htt antibodies described above.

3.2. Detection of *Cj-Htt* gene products

It is important to be able to properly detect the *Cj-Htt* gene and its gene products. Since the nucleotide and predicted amino acid sequences of the *Cj-Htt* cDNA showed significantly high sequence homologies to those of the human *Htt* gene, we tested whether commercially-available TaqMan probe and antibodies against human *Htt* gene products (mRNA and protein) were also able to detect *Cj-Htt* gene products. As a result, the TaqMan probe (Fig. 5A) appears to be able to detect *Cj-Htt* mRNA. In addition, newly designed PCR primers, which are perfectly matched to *Cj-Htt*, also appear to be able to detect *Cj-Htt* mRNA (Fig. 5B).

Fig. 4. Gene silencing against the 5′*Cj-Htt-GFP* fusion gene. (A) Schematic drawing of the 5′*Cj-Htt-GFP* fusion gene and designed cjHtt-1 siRNA. The fusion gene is composed of the 5′ terminal region of the Cj-Htt ORF and GFP, and driven by the Human cytomegalovirus promoter. The *Cj-Htt* sequence from the first ATG to position 50 is shown together with sequences of cjHtt-1 siRNA and siRNA-HDexon1 targeting human *Htt*. A variant nucleotide between the siRNAs is indicated in red. (B) Effect of cjHtt-1 siRNA on gene silencing. Reporter genes [5′*Cj-Htt-GFP* or *GFP* (empty reporter)] and siRNAs [cjHtt-1 or siCont (non-silencing siRNA)] were introduced into mouse neuroblastoma Neuro2a (N2a) cells. Two days after transfection, the cells were examined by a fluorescent microscope. Left (differential interference contrast) and right (fluorescence image) panels are identical in the visual field.

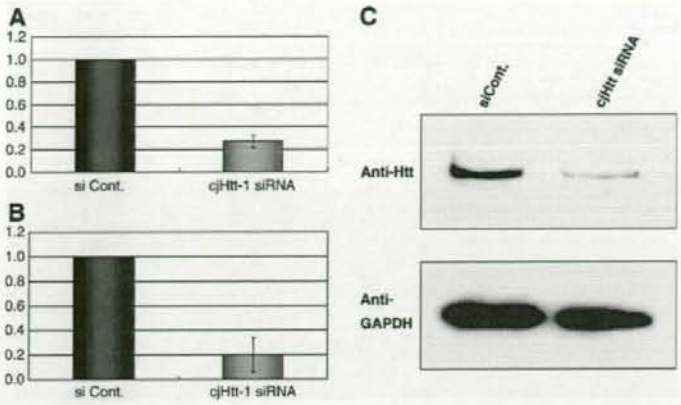

Fig. 5. Inhibition of expression of endogenous *Cj-Htt* by RNAi. The cjHtt-1 siRNA was introduced into HSCj-009 cells by means of electroporation. Two days after transfection, total RNA and cell lysate were prepared and examined by RT-real time PCR and Western blotting, respectively. Total RNA was subjected to cDNA synthesis as in Fig. 1. The resultant cDNA was examined by real time PCR with a TaqMan probe for the human *Htt* gene (A) and newly designed PCR primers [cjHtt(1139)-F and cjHtt(1254)-R] (B). The expression of *Gapdh* as a control was also examined using Perfect Real Time Primers for the human *GAPDH* gene (TAKARA BIO). The expression level of *Cj-Htt* was normalized against that of *Gapdh*, and the ratios of *Cj-Htt* expression level in the presence of cjHtt-1 siRNA were normalized against the ratio obtained in the presence of the siControl siRNA (siCont.). Data are means of at least three independent determinations. Error bars represent standard deviations. (C) Western blot. Cell lysate was examined by Western blotting with anti-human Htt antibody (MAB2166; Chemicon) as in Fig. 3. After detection of signals, the expression of GAPDH as a control was also examined by anti-GAPDH antibody (AM4300; Ambion).

Western blot analyses indicate that a polypeptide of approximately 350 kDa, which is almost the same as the molecular weight estimated from the amino acid sequence (346 kDa) in the *Cj-Htt* cDNA, can be detected in the common marmoset specimens by the antibodies tested, suggesting that the Cj-Htt protein is detectable with the antibodies (Figs. 3A–C). The 350 kDa mouse Htt protein was detected by the MAB2166 antibody (Fig. 3A), but hardly with the other antibodies (Figs. 3B and C). This may be caused by possibly low expression level of mouse Htt in the brain tissue, and/or by difference in the epitope sequences between the common marmoset and mouse Htt proteins. Other than the 350 kDa band, a few bands migrated faster than the 350 kDa band were also observed. They may be degradation products of the Htt protein, and different cells and/or species might have different degradation of the protein. To clarify these, further studies need to be carried out.

In addition to the Htt protein, we also examined the expression of amyloid precursor protein (App) with the 22C11 antibody, which can recognize the same amino acid sequence at positions 66–81 of either the human or mouse App. As a result, the App signal was able to be detected in either the common marmoset or mouse brain tissue, but not in the common marmoset immortalized peripheral blood mononuclear cells (PBMCs) (Fig. 3D), suggesting little or no expression of App in PBMCs and availability of the antibody for detection of the Cj-App protein.

3.3. *Gene silencing against the Cj-Htt gene*

To verify the data presented here and tools for the detection of *Cj-Htt*, we carried out gene silencing against the expression of endogenous *Cj-Htt* by means of RNA interference (RNAi), and assessed the knockdown potency of designed siRNA targeting *Cj-Htt* using the tools evaluated above. Based on a previous study where a competent siRNA duplex, siRNA-HDexon 1, conferring strong inhibition against the expression of the human *Htt* gene was used (Liu et al., 2003), we chemically synthesized an siRNA duplex, cjHtt-1 siRNA, corresponding to the siRNA-HDexon 1 duplex; note that there is one nucleotide change between cjHtt-1 siRNA and siRNA-HDexon 1 (Fig. 4A).

To examine the effect of the siRNA duplex on gene silencing, we constructed a reporter plasmid carrying the 5′ terminal region of *Cj-Htt* cDNA linked with the *GFP* reporter gene (the 5′*Cj-Htt-GFP* fusion gene). The reporter plasmid and the siRNA were cotransfected into mouse Neuro2a cells, and the expression of the 5′*Cj-Htt-GFP* fusion gene was examined by a fluorescent microscope. As shown in Fig. 4B, the data indicated that the cjHtt-1 siRNA duplex was able to induce strong RNAi activity against the fusion gene expression.

Next, we introduced the cjHtt-1 siRNA duplex into immortalized common marmoset mononuclear cells by means of electroporation, and two days after transfection, the expression levels of the endogenous *Cj-Htt* mRNA and protein were examined by RT-real time PCR and Western blotting, respectively. As shown in Fig. 5, the results consistently indicated that *Cj-Htt* mRNA (A and B) and protein (C) levels markedly decreased in the presence of the cjHtt-1 siRNA duplex, i.e., potent RNAi knockdown against the endogenous *Cj-Htt* gene was induced by the siRNA duplex. Finally, the data presented here also indicate that proper detection of the newly identified *Cj-Htt* gene and its products can be performed by means of the methods and tools assessed in this study.

In conclusion, we described for the first time the common marmoset *Htt* gene, and also detection methods and tools for the gene and its gene products. The data presented here may assist us in promoting a non-human primate HD model with the common marmoset.

Acknowledgments

We would like to thank Dr. R.C. Desrosiers for kindly providing HS viruses. We also thank Drs. K. Nakamura, T. Kabuta, M. Suzuki, and C. Konya for their helpful advice and discussion. Finally, we would like to thank Dr I. Kanazawa for his encouragement and helpful advice. This work was supported by research grants from the Ministry of Health, Labour and Welfare of Japan.

References

Akari, H., et al., 1996. In vitro immortalization of Old World monkey T lymphocytes with Herpesvirus saimiri: its susceptibility to infection with simian immunodeficiency viruses. Virology 218, 382–388.

Andrade, M.A., Bork, P., 1995. HEAT repeats in the Huntington's disease protein. Nat. Genet. 11, 115–116.

Deisboeck, T.S., et al., 2003. Development of a novel non-human primate model for preclinical gene vector safety studies. Determining the effects of intracerebral HSV-1 inoculation in the common marmoset: a comparative study. Gene Ther. 10, 1225–1233.
Doods, H., et al., 2000. Pharmacological profile of BIBN4096BS, the first selective small molecule CGRP antagonist. Br. J. Pharmacol. 129, 420–423.
Gilliam, T.C., et al., 1987. A DNA segment encoding two genes very tightly linked to Huntington's disease. Science 238, 950–952.
Gusella, J.F., et al., 1983. A polymorphic DNA marker genetically linked to Huntington's disease. Nature 306, 234–238.
Huntington's-Disease, C.R.G.o., The Huntington's Disease Collaborative Research Group, 1993. A novel gene containing a trinucleotide repeat that is expanded and unstable on Huntington's disease chromosomes. Cell 72, 971–983.
Kazemi-Esfarjani, P., Benzer, S., 2000. Genetic suppression of polyglutamine toxicity in Drosophila. Science 287, 1837–1840.
Kendall, A.L., Rayment, F.D., Torres, E.M., Baker, H.F., Ridley, R.M., Dunnett, S.B., 1998. Functional integration of striatal allografts in a primate model of Huntington's disease. Nat. Med. 4, 727–729.
Liu, W., Goto, J., Wang, Y., Murata, M., Wada, K., Kanazawa, I., 2003. Specific inhibition of Huntington's disease gene expression by siRNAs in cultured cells. Proc. Jpn. Acad. 79, 293–298.
Lunkes, A., Mandel, J.L., 1998. A cellular model that recapitulates major pathogenic steps of Huntington's disease. Hum. Mol. Genet. 7, 1355–1361.
Mangiarini, L., et al., 1996. Exon 1 of the HD gene with an expanded CAG repeat is sufficient to cause a progressive neurological phenotype in transgenic mice. Cell 87, 493–506.
Neuwald, A.F., Hirano, T., 2000. HEAT repeats associated with condensins, cohesins, and other complexes involved in chromosome-related functions. Genome Res. 10, 1445–1452.
Palfi, S., et al., 2007. Expression of mutated huntingtin fragment in the putamen is sufficient to produce abnormal movement in non-human primates. Mol. Ther. 15, 1444–1451.
Sakai, T., Hohjoh, H., 2006. Gene silencing analyses against amyloid precursor protein (APP) gene family by RNA interference. Cell Biol. Int. 30, 952–956.
t'Hart, B.A., Vervoordeldonk, M., Heeney, J.L., Tak, P.P., 2003. Gene therapy in nonhuman primate models of human autoimmune disease. Gene Ther. 10, 890–901.
von Horsten, S., et al., 2003. Transgenic rat model of Huntington's disease. Hum. Mol. Genet. 12, 617–624.
Walker, F.O., 2007. Huntington's disease. Lancet 369, 218–228.
Yang, S.H., et al., 2008. Towards a transgenic model of Huntington's disease in a non-human primate. Nature 453, 921–924.

Retrovirology

BioMed Central

Research

Open Access

MDM2 is a novel E3 ligase for HIV-1 Vif

Taisuke Izumi[1], Akifumi Takaori-Kondo*[1], Kotaro Shirakawa[1,2], Hiroaki Higashitsuji[3], Katsuhiko Itoh[3], Katsuhiro Io[1], Masashi Matsui[1], Kazuhiro Iwai[4,5], Hiroshi Kondoh[6], Toshihiro Sato[7], Mitsunori Tomonaga[7], Satoru Ikeda[7], Hirofumi Akari[8], Yoshio Koyanagi[9], Jun Fujita[3] and Takashi Uchiyama[1]

Address: [1]Department of Hematology and Oncology, Graduate School of Medicine, Kyoto University, 54 Shogoin-Kawaracho, Sakyo-ku, Kyoto 606-8507, Japan, [2]Japanese Foundation for AIDS Prevention, 1-3-12 Misaki-cho, Chiyoda-ku, Tokyo 101-0061, Japan, [3]Department of Clinical Molecular Biology, Graduate School of Medicine, Kyoto University, 54 Shogoin-Kawaracho, Sakyo-ku, Kyoto 606-8507, Japan, [4]Department of Molecular Cell Biology, Graduate School of Medicine, Osaka City University, 1-4-3 Asahi-machi, Abeno-ku, Osaka 545-8585, Japan, [5]CREST, Japan Science Technology Corporation, Kawaguchi, Saitama 332-0012, Japan, [6]Department of Geriatric Medicine, Graduate School of Medicine, Kyoto University, 54 Shogoin-Kawaracho, Sakyo-ku, Kyoto 606-8507, Japan, [7]Central Pharmaceutical Research Institute, Japan Tobacco Inc., 1-1 Murasaki-cho, Takatsuki, Osaka 569-1125, Japan, [8]Laboratory of Disease Control, Tukuba Primate Research Center, National Institute of Biomedical Innovation, Hachimandai-1, Tsukuba, Ibaraki 305-0843, Japan and [9]Laboratory of Viral Pathgenesis, Institute for Virus Research, Kyoto University, 53 Shogoin-Kawaracho, Sakyo-ku, Kyoto 606-8507, Japan

Email: Taisuke Izumi - izumi.t@aw3.ecs.kyoto-u.ac.jp; Akifumi Takaori-Kondo* - atakaori@kuhp.kyoto-u.ac.jp; Kotaro Shirakawa - kotash@kuhp.kyoto-u.ac.jp; Hiroaki Higashitsuji - hhigashi@virus.kyoto-u.ac.jp; Katsuhiko Itoh - katsu@virus.kyoto-u.ac.jp; Katsuhiro Io - katsu829@kuhp.kyoto-u.ac.jp; Masashi Matsui - mmatsui@kuhp.kyoto-u.ac.jp; Kazuhiro Iwai - kiwai@cellbio.med.osaka-u.ac.jp; Hiroshi Kondoh - hkondoh@kuhp.kyoto-u.ac.jp; Toshihiro Sato - toshihiro.sato@ims.jti.co.jp; Mitsunori Tomonaga - mitsunori.tomonaga@ims.jti.co.jp; Satoru Ikeda - satoru.ikeda@ims.jti.co.jp; Hirofumi Akari - akari@nibio.go.jp; Yoshio Koyanagi - ykoyanag@virus.kyoto-u.ac.jp; Jun Fujita - jfujita@virus.kyoto-u.ac.jp; Takashi Uchiyama - uchiyata@kuhp.kyoto-u.ac.jp

* Corresponding author

Published: 7 January 2009

Retrovirology 2009, **6**:1 doi:10.1186/1742-4690-6-1

Received: 16 September 2008
Accepted: 7 January 2009

This article is available from: http://www.retrovirology.com/content/6/1/1

Abstract

The human immunodeficiency virus type 1 (HIV-1) Vif plays a crucial role in the viral life cycle by antagonizing a host restriction factor APOBEC3G (A3G). Vif interacts with A3G and induces its polyubiquitination and subsequent degradation via the formation of active ubiquitin ligase (E3) complex with Cullin5-ElonginB/C. Although Vif itself is also ubiquitinated and degraded rapidly in infected cells, precise roles and mechanisms of Vif ubiquitination are largely unknown. Here we report that MDM2, known as an E3 ligase for p53, is a novel E3 ligase for Vif and induces polyubiquitination and degradation of Vif. We also show the mechanisms by which MDM2 only targets Vif, but not A3G that binds to Vif. MDM2 reduces cellular Vif levels and reversely increases A3G levels, because the interaction between MDM2 and Vif precludes A3G from binding to Vif. Furthermore, we demonstrate that MDM2 negatively regulates HIV-1 replication in non-permissive target cells through Vif degradation. These data suggest that MDM2 is a regulator of HIV-1 replication and might be a novel therapeutic target for anti-HIV-1 drug.

Background

Host restriction factors protect hosts from viruses, whereas viruses evade these proteins to replicate more efficiently in host cells. The interplay between the host restriction factors and viral proteins is therefore very important for regulating viral replication [1,2]. A3G (Apolipoprotein B mRNA editing enzyme, catalytic polypeptide-like 3G) is a newly identified anti-HIV-1 host factor [3], which belongs to the APOBEC superfamily of cytidine deaminases, consisting of APOBEC1, APOBEC2, AID (activation-induced cytidine deaminase), APOBEC3(A-H), and APOBEC4 [4]. A3G is incorporated into HIV-1 virions and inhibits HIV-1 replication by inducing G-to-A hypermutation in viral cDNA during reverse transcription [5-8]. HIV-1 Vif counteracts A3G by targeting it for proteasomal degradation, thus supporting HIV-1 replication in non-permissive target cells [9-11]. Vif forms a ubiquitin ligase (E3) complex with Cullin5 (Cul5), Elongin B, and Elongin C and functions as a substrate recognition subunit of this complex to induce ubiquitination and subsequent degradation of A3G [12,13]. Vif also counteracts several APOBEC3 proteins including APOBEC3F (A3F) [14,15]. These observations reconcile the long-standing mystery of why Vif function is necessary for HIV-1 to infect non-permissive cells. On the other hand, it has been shown that intracellular levels of Vif are maintained relatively low by ubiquitination in virus-producing cells [16-18]. Although several groups have reported E3 ligases important for Vif ubiquitination [17,18], the precise roles and mechanisms of Vif ubiquitination remain unclear. Here we demonstrate that MDM2 is a novel E3 ligase for Vif and that it induces ubiquitination and degradation of Vif, thereby regulating HIV-1 replication.

Results

MDM2 downregulates cellular Vif levels by inducing its degradation in a proteasome-dependent manner

To investigate the biological roles and molecular mechanisms of Vif ubiquitination, we tried to identify a novel E3 ligase that may be involved in the ubiquitination of Vif. During a search for Vif-interacting proteins in the HIV, Human Protein Interaction Database of National Institute for Allergy & Infectious Diseases http://www.ncbi.nlm.nih.gov/RefSeq/HIVInteractions/, we were struck by a protein called Gankyrin (proteasome 26S subunit, non-ATPase, 10 (PSMD10)). We first examined the biological effects of Gankyrin, but could not detect a downregulation of Vif (data not shown). As we previously reported that Gankyrin itself doesn't have an enzymatic activity and that it rather enhances the E3 ligase activity of MDM2 on p53 ubiquitination and degradation as a co-factor [19], we tested the possibility that MDM2 plays an important role in Vif ubiquitination as a novel E3 ligase. We examined the effect of several E3 ligases including MDM2 (a RING finger type E3 that mediates p53 ubiquitination and degradation [20]), Cul5 (another RING finger type E3 that forms a complex with Vif and is reported to induce Vif ubiquitination [17,21]), and Parkin (another RING finger type E3) on cellular Vif levels (Fig. 1A). HEK293T cells were transfected with a subgenomic expression vector pNL-A1 that expressed all HIV-1 proteins except for *gag* and *pol* products [22], together with the expression plasmids for these E3 ligases. We found that the ectopic expression of MDM2 downregulated the cellular levels of Vif as well as p53 in transfected cells in a dose-dependent manner (Fig. 1A, lanes 8–10), whereas Parkin and Cul5 did not affect their cellular levels (lanes 2–4 and 5–7, respectively), even though the latter proteins were expressed more than MDM2. Our results are discrepant with previous reports that demonstrated Cul5 induced Vif ubiquitination and degradation [17,23]. We assume that overexpression of Cul5 alone is insufficient to induce Vif degradation, because other E3 components are not overexpressed. Ectopic expression of MDM2 did not affect cellular levels of another viral protein such as Nef, suggesting that MDM2 specifically downregulated Vif levels; this result also excluded the possibility that MDM2 affected the transcriptional activity of the HIV-1 LTR.

Because it is well known that MDM2 regulates p53 levels by modulating its protein stability, we next examined the protein stability of Vif with the ectopic expression of MDM2. HEK293T cells were transfected with pNL-A1 with or without a MDM2 expression vector and treated with cycloheximide 21 hrs after transfection. After cycloheximide treatment, cellular levels of Vif decreased by 60% in MDM2-transfected cells and by 20% in control cells, respectively (Fig. 1B &1C), indicating that Vif decayed much faster when MDM2 was overexpressed. The stability profile of Vif protein was similar to that of p53 (Fig. 1B). However, in our hands, the half-life of Vif protein was longer than those shown in previous studies from several laboratories. We interpret that this difference is attributable to divergent methods used in the studies which employed radioisotopes or cycloheximide. Thus, our findings suggest that MDM2 affects the stability of Vif protein similar to its effect on p53. We also examined the stability of Vif in MDM2-/- MEF cells. Vif decayed much faster in p53-/- MEF cells than in p53-/-MDM2-/- double knock-out (DKO) MEF cells (Additional file 1), suggesting that endogenous MDM2 can also influence the stability of Vif. We then tested a RING finger domain-deleted MDM2 mutant, ΔRF, which is inactive for the ubiquitination activity of MDM2 [24]. Ectopic expression of MDM2 suppressed cellular Vif levels, but the expression of ΔRF did not (Fig. 1D). This result suggests that ubiquitination of Vif by MDM2 is involved in the downregulation of cellular Vif levels. We further treated transfected cells with a proteasome inhibitor MG132 to see whether the down-

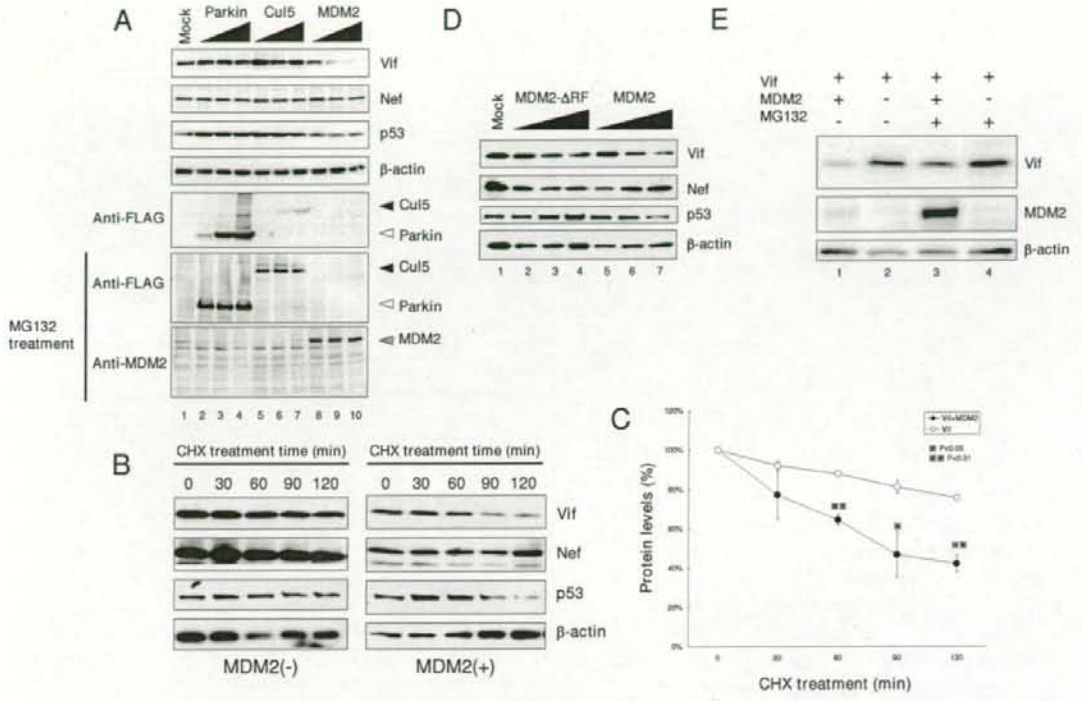

Figure 1

MDM2 downregulated cellular Vif levels in a proteasome dependent manner. (A) MDM2 reduced cellular levels of Vif as well as p53, but not that of Nef. HEK293T cells were cotransfected with expression vectors for the indicated E3 ligases and a subgenomic HIV-1 expression vector pNL-A1. Cell lysates were subjected to immunoblotting with the indicated Abs. We could not detect the expression of FLAG-MDM2 without MG132 treatment, because of a rapid degradation of MDM2. MG132 treatment enabled us to detect expression of MDM2 only with anti-MDM2 Ab, but not with anti-FLAG mAb. (B) Twenty-two hours after transfection, the cells were treated with cycloheximide (CHX)(80 μg/ml) for the indicated times, and cell lysates were subjected to immunoblotting with the indicated Abs. (C) The amounts of Vif and Nef were quantified by densitometry, and Vif protein levels were calculated using Nef protein levels as normalizing loading controls and presented as percentage values relative to that without CHX treatment set as 100%. Values are presented as averages of three independent experiments. (D) MDM2 downregulated Vif, but a ΔRF mutant did not. HEK293T cells were cotransfected with expression vectors for MDM2 and the mutant together with pNL-A1, and cell lysates were subjected to immunoblotting with the indicated Abs. (E) $p53^{-/-}MDM2^{-/-}$ DKO-MEF cells were cotransfected with expression vectors for MDM2 and Vif, and treated with 10 μM MG132 for 6 hrs, and cell lysates were subjected to immunoblotting with the indicated Abs.

regulation of Vif by MDM2 was proteasome-dependent. Treatment with MG132 clearly restored the cellular Vif level that was downregulated by MDM2 (Fig. 1E, top panel, lane 3 as compared with lane 1), supporting that the MDM2-mediated downregulation of Vif was proteasome-dependent. Taken together, we concluded that MDM2 downregulates cellular Vif level by inducing its degradation in a proteasome-dependent manner.

MDM2 specifically binds and downregulates Vif

To further investigate the molecular link between MDM2 and Vif, we next examined the physical interaction of MDM2 with Vif. Immunoprecipitation assays showed that Vif was co-precipitated with MDM2 (Fig. 2A). Glutathione S-transferase (GST) pull-down assays showed that MDM2 was found in GST-Vif-bound, but not GST-bound, material (data not shown). Using a series of MDM2 deletion mutants, we determined that the central region of MDM2 (amino acids 168–320) was necessary for Vif binding (Fig. 2B, left panel &2C). To more precisely

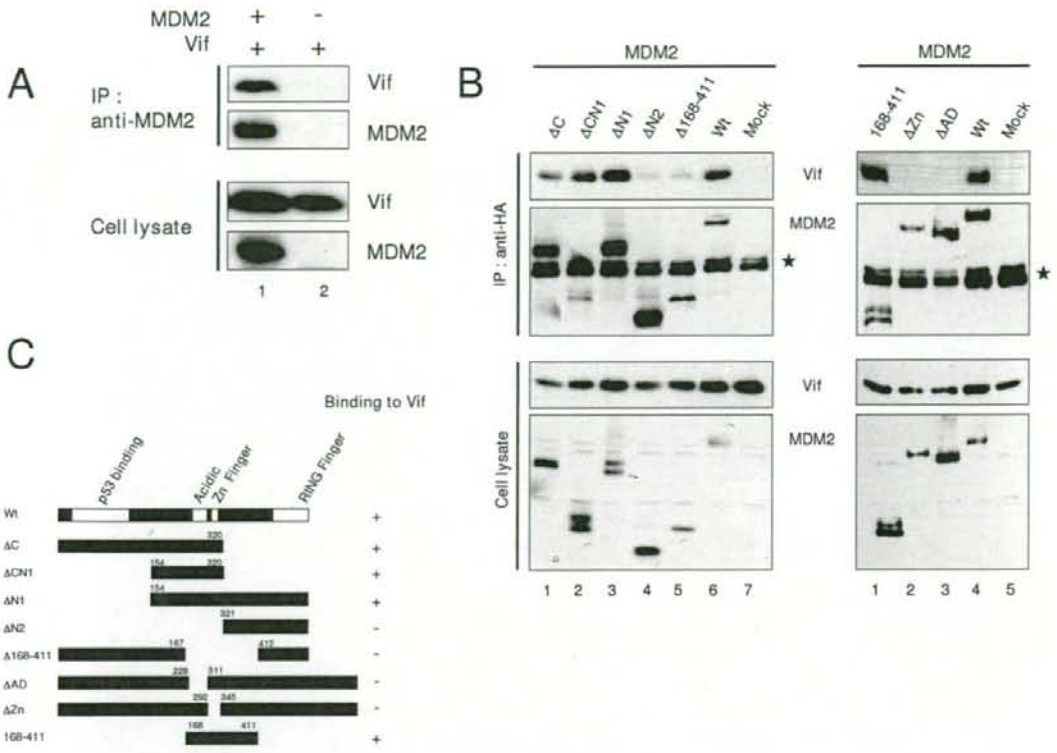

Figure 2

MDM2 bound Vif in its central domain. (A) Immunoprecipitation assays revealed the interaction of MDM2 with Vif *in vivo*. HEK293T cells were cotransfected with expression vectors for MDM2 and Vif and treated with MG132 for 6 hrs prior to harvest. Cell lysates were immunoprecipitated with anti-MDM2 mAb followed by immunoblotting with the indicated Abs (upper two panels). Cell lysates were also subjected to immunoblotting with the indicated Abs (lower two panels). (B) The interaction domain of MDM2 with Vif. HEK293T cells were cotransfected with expression vectors for HA-tagged MDM2 wild type (Wt) and mutants together with pNL-A1, and cell lysates were immunoprecipitated with anti-HA mAb followed by immunoblotting with the indicated Abs. Asterisk indicates immunoglobulin heavy chains from thenimmunoprecipitation. (C) Schematics of MDM2 mutants binding to Vif are shown.

determine a Vif-binding domain, we further tested mutants deleted in a Zn Finger domain (ΔZn) or in an acidic domain (ΔAD). Neither mutant could bind Vif, whereas the mutant containing amino acids 168–411 was able to bind Vif, suggesting that both domains are necessary and that the central domain is sufficient for Vif binding (Fig. 2B, right panel &2C). Additionally, using a series of Vif deletion mutants, we also found that the N-terminal region of Vif (amino acids 4–22) is needed for MDM2 binding (Fig. 3A &3C). Furthermore, we examined the MDM2-mediated downregulation of Vif mutants. MDM2 was able to efficiently downregulate cellular levels of the MDM2-binding Vif mutants but not that of an MDM2-non binding mutant, Δ4–45 (Fig. 3B). Collectively, these results indicated that the Vif-MDM2 interaction is required for MDM2-mediated downregulation of Vif (Fig. 3C).

MDM2 induces ubiqutination of Vif

Since we found that MDM2 bound Vif and promoted its degradation via a proteasomal pathway, we next examined whether MDM2 is involved in the polyubiquitination of Vif. *In vitro* ubiquitination assays revealed that bacterially expressed GST-MDM2 was able to induce the

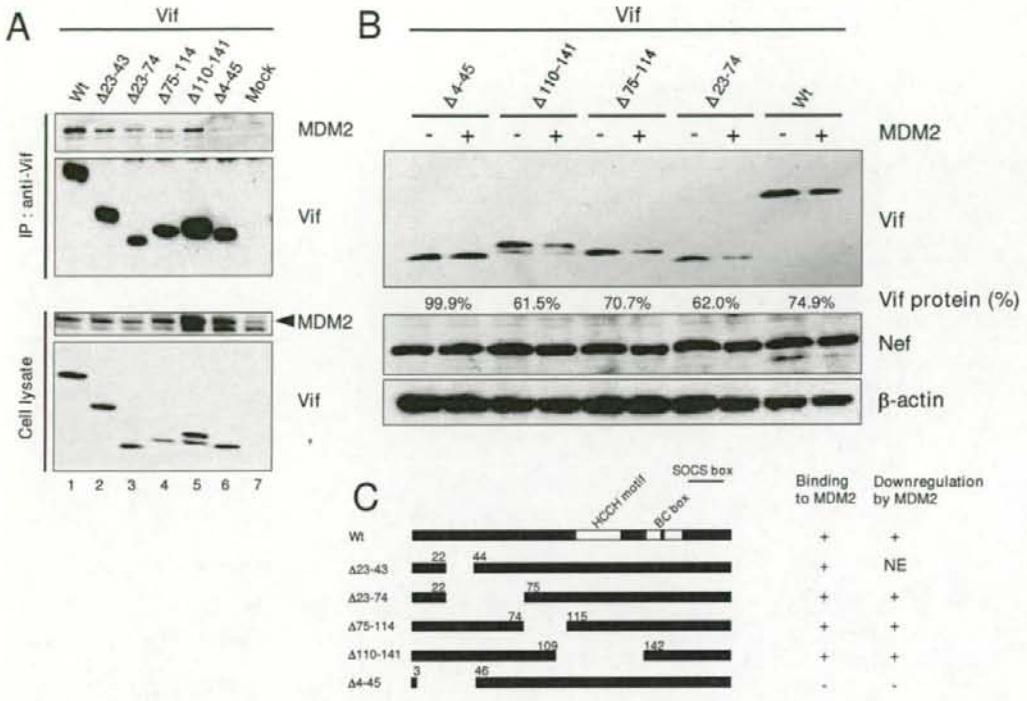

Figure 3

MDM2 specifically bound and downregulated Vif. (A) The interaction domain of Vif with MDM2. HEK293T cells were cotransfected with expression vectors for Vif and mutants together with pCMV/HA-MDM2, and cell lysates were immunoprecipitated with anti-Vif mAb followed by immunoblotting with the indicated Abs. Arrowhead indicates MDM2. (B) The downregulation of Vif protein by MDM2. HEK293T cells were cotransfected with expression vectors for Vif and mutants with or without pCMV/HA-MDM2, and cell lysates were subjected to immunoblotting with the indicated Abs. The amounts of Vif were quantified by densitometry and shown as the protein ratio relative to that without expression of MDM2. (C) Schematics of Vif mutants bound by and downregulated by MDM2. NE: not examined.

polyubiquitination of purified GST-Vif protein *in vitro* (Fig. 4A). The ubiquitination of Vif by MDM2 was specific, as the omission of ubiqutin, E1, E2, or MDM2 prevented Vif-ubiquitination as shown in our previous experiments [13]. We also performed *in vitro* ubiquitination assays using immunopurified MDM2 and Cul5. Immunopurified MDM2 was able to induce ubiquitination of Vif *in vitro* to the same extent as Cul5 (Additional file 2, part A), while it could not ubiquitinate the N-terminal Vif deletion mutant Δ22 that was defective for binding MDM2 (Additional file 2, part B). These findings suggest that the interaction with MDM2 is important for Vif ubiquitination. We performed *in vivo* ubiquitination assays to further investigate the importance of MDM2 in Vif ubiquitination. Lysates of cells co-expressing Vif, either with an MDM2 wild type (Wt) or a ΔRF mutant, and His-tagged Ubiquitin (His-Ub) were analyzed for the presence of ubiquitinated Vif conjugates (Fig. 4B). Unfortunately, we detected a Vif band that non-specifically bound to Ni-NTA agarose (arrowhead) due to its nature as a sticky protein. Overexpression of MDM2 induced a ladder detected by anti-Vif Ab, even in the absence of His-Ub (lane 2), suggesting that this ladder represented Vif protein polyubiquitinated with endogenous Ub (arrows with asterisk). Furthermore, in the presence of His-Ub, we detected a doublet of ladder which presumably represented Vif protein polyubiquitinated with endogenous and His-tagged Ub (arrows with asterisk and arrows, respectively). We also obtained similar results using a UbiQapture™-Q Kit (data not shown). We thus concluded that the overexpres-

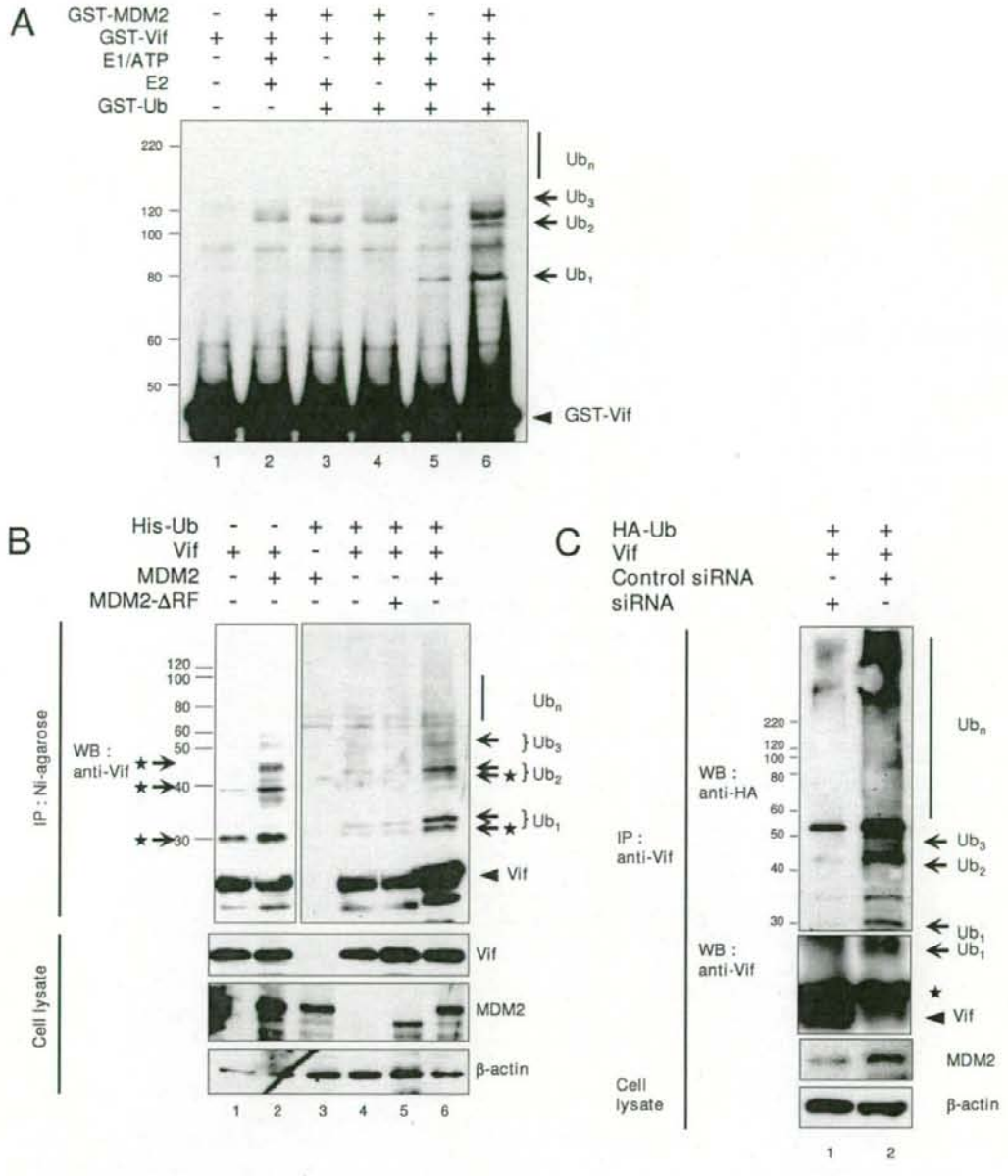

Figure 4 *(see legend on next page)*

Figure 4 *(see previous page)*
MDM2 induced the polyubiquitination of Vif *in vitro* and *in vivo*. (A) GST-MDM2 induced the polyubiquitination of Vif *in vitro*. Bacterially expressed GST-Vif was subjected to *in vitro* ubiquitination assays. The reaction was performed in the presence or absence of E1, E2, GST-MDM2, and GST-Ubiquitin as indicated. Reactions were subjected to immunoblotting with anti-Vif mAb. Arrows indicate GST-ubiquitin-conjugated Vif. (B) Overexpressed MDM2 induced the polyubiquitination of Vif *in vivo*. HEK293T cells were cotransfected with expression vectors for MDM2 Wt and a ΔRF mutant together with expression vectors for Vif and His-Ubiquitin (His-Ub) as indicated. Cells were treated with MG132 for 6 hrs, and cell lysates were precipitated with Ni-NTA agarose beads followed by immunoblotting with the indicated Abs. Since Vif naturally bound to Ni-NTA agarose, we detected a Vif band itself (arrowhead), whereas no signal was detected in cells lacking Vif (lane 3). Arrows indicate His-Ub-conjugated Vif. Arrows with asterisk indicate Vif conjugated with endogenous ubiquitin. (C) Transduction of siRNA reduced cellular levels of endogenous MDM2 and polyubiquitination of Vif. HEK293T cells were cotransfected with expression vectors for MDM2 siRNA and control siRNA together with expression vectors for Vif and HA-Ubiquitin (HA-Ub). Cell lysates were immunoprecipitated with anti-Vif mAb followed by immunoblotting with the indicated Abs. Asterisk indicates immunoglobulin light chains from the immunoprecipitation.

sion of exogenous MDM2 efficiently induced polyubiquitination of Vif *in vivo*. Furthermore, the knock-down of endogenous MDM2 expression by introduction of MDM2-specific short interfering RNA (siRNA) resulted in a significant reduction in the amount of polyubiquitinated Vif, commensurate with the extent of reduced MDM2 expression (Fig. 4C). Collectively, these data indicated that MDM2 mediates polyubiquitination of Vif both *in vitro* and *in vivo*.

MDM2 negatively regulates HIV-1 replication in non-permissive cells through ubiqutination and degradation of Vif

Next, we examined the effect of MDM2 on HIV-1 replication. In a single round infection assay (Fig. 5A), in the absence of A3G, viral replication was not affected by expression of MDM2 and/or Vif (lanes 1–6). In contrast, in the presence of A3G in a non-permissive cell setting, without the expression of MDM2, the wild type virus could replicate but the ΔVif virus could not, as previously reported (lanes 7 & 8) [3,8]. Co-expression of MDM2 reduced the cellular level of Vif (Fig. 5B, upper panel, lanes 5 & 11), resulting in the increased virion incorporation of A3G (Fig. 5B, 2nd lower panel, lane 11 as compared with lanes 7) and the greater suppression of viral replication (Fig. 5A, lane 11 as compared with lane 7).

We also tested the effect of MDM2 on HIV-1 replication in the presence of A3F. MDM2 suppressed viral replication in the presence of A3F, similar to results shown for A3G (Additional file 3). These data indicated that the MDM2-mediated Vif downregulation led to upregulated cellular A3G and A3F levels in producer cells, resulting in less infectious HIV-1 virions produced. Since MDM2 was previously reported to upregulate HIV-1 transcription by ubiquitination of Tat, we further examined HIV-1 replication in macrophages knocked down for MDM2 (Fig. 5C). We chose terminally differentiated macrophages as the target, because the knockdown of MDM2 is lethal for proliferating cells. HIV-1 replicated more efficiently in macrophages transfected with MDM2 siRNA than in control siRNA-transfected macrophages. These data indicated that MDM2 negatively regulated HIV-1 replication in non-permissive target cells through the ubiquitination and degradation of Vif.

To obtain further insights into the mechanisms why our MDM2 system did not induce the ubiquitination of A3G which was bound to Vif, we tested the expression levels and the binding affinity of A3G to Vif in transfected cells. Co-expression of MDM2 reduced the cellular levels of Vif and inversely increased the A3G levels in a dose dependent manner (Fig. 5D). Immunoprecipitation assays revealed that the co-expression of MDM2 blocked the binding of A3G to Vif in a dose dependent manner (Fig. 5E). These data suggest that the interaction between MDM2 and Vif precludes A3G from binding to Vif.

Discussion

In this study, we report that MDM2 is a novel E3 ligase for HIV-1 Vif. MDM2 physically interacts with Vif and functions as an E3 ligase for Vif to induce its polyubiquitination and proteasomal degradation. Several E3 ligases including Cul5 [17], Nedd4, and AIP4 [18], have been reported to induce Vif ubiquitination, and the roles of Cul5 for Vif ubiquitination and degradation are especially well documented. Dang et al. have recently reported that Cul5 induces A3G degradation not by direct ubiquination of A3G but indirectly through Vif ubiqutination and that polyubiquitinated Vif might serve as a vehicle to transport A3G into proteasomes for degradation [23]. In this manuscript, we show that MDM2 only targets Vif for degradation but not A3G, although MDM2 and Cul5 both induce Vif ubiquitination (Additional file 2, part A). MDM2 reduced cellular Vif levels and inversely increased A3G levels (Fig. 5B &5D), unlike Cul5. One possible explanation is that the binding of MDM2 to Vif precluded A3G from binding Vif (Fig. 5E), whereas a Cul5-Vif complex

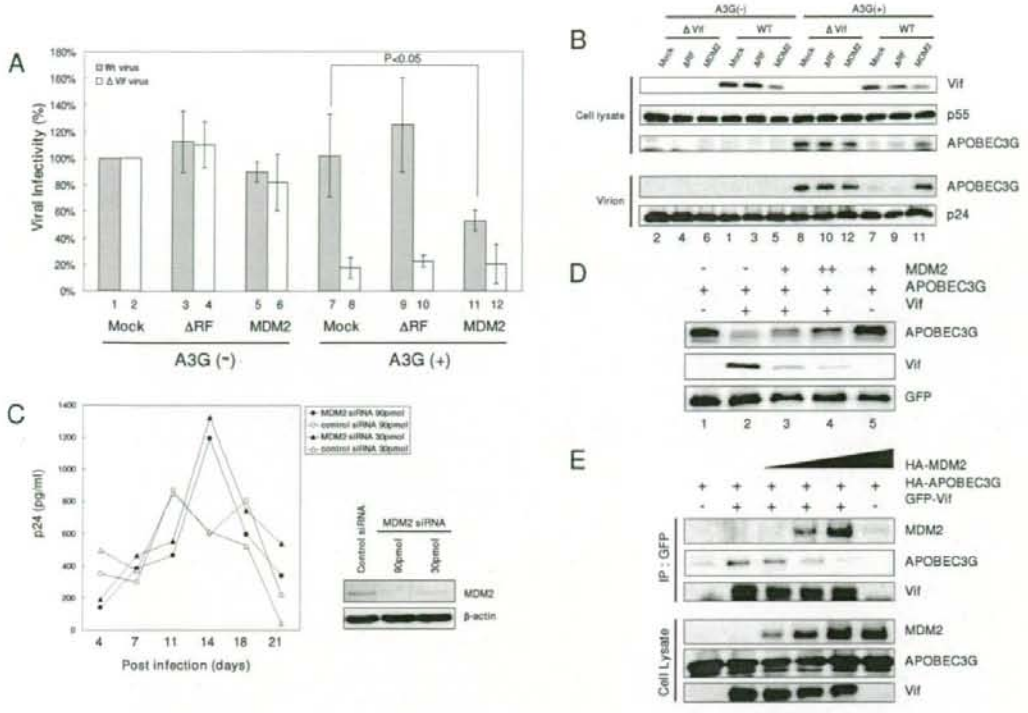

Figure 5

MDM2 negatively regulated HIV-1 replication in non-permissive cells through the degradation of Vif. (A) The overexpression of MDM2 inhibited HIV-1 replication in the presence of A3G. NL-43 Wt and ΔVif viruses were produced from HEK293T cells transfected with expression vectors for MDM2 Wt and a ΔRF mutant in the presence or absence of A3G. The viral infectivity was examined using M8166 cells. Values are presented as averages of more than 3 independent experiments. (B) MDM2 reduced cellular levels of Vif, resulting in more incorporation of A3G into HIV-1 virions. Immunoblotting for cell lysates (upper 3 panels) and precipitated virions (lower 2 panels) was performed with the indicated Abs. Lane numbers correspond to those in Fig. 4A. (C) HIV-1 replication in macrophages transfected with MDM2- and control-siRNA. MDM were transfected with MDM2- and control-siRNA and challenged with R5 HIV-1_{JR-FL} (left panel). Cell lysates were subjected to immunoblotting with the indicated antibodies (right panels). (D) Coexpression of MDM2 reduced cellular levels of Vif and inversely increased A3G levels in a dose dependent manner. HEK293T cells were cotransfected with expression vectors for A3G, Vif, GFP, and MDM2 as indicated. Cell lysates were subjected to immunoblotting with the indicated Abs. (E) Immunoprecipitation assays revealed that the coexpression of MDM2 blocked the binding of A3G to Vif in a dose dependent manner. HEK293T cells were cotransfected with expression vectors for A3G, GFP-Vif, and MDM2 as indicated. Cell lysates were immunoprecipitated with anti-GFP mAb followed by immunoblotting with the indicated Abs.

can bind A3G to form a ternary complex. MDM2 binds the N-terminal region of Vif which does not overlap with, but is close to the A3G/A3F binding domain [25]. This binding might affect the interaction of Vif with A3G and/or A3F. Furthermore, the evidence that an MDM2 ΔRF mutant failed to protect A3G indicated that the ubiquitination and degradation of Vif is necessary to protect A3G and A3F from Vif. These findings suggest that different E3 ligases might play different roles in Vif ubiquitination. Further studies on the different roles of Vif ubiquitination by different E3 ligases and their virological significance should be investigated.

We demonstrate that MDM2 negatively regulated HIV-1 replication through Vif degradation. Through the degradation of target proteins (p53, pRB, etc), MDM2 can exert profound physiological effects on the regulation of cell cycle, cell proliferation, DNA repairs and other processes. To our knowledge, this is the first report to show that MDM2 plays an important role in viral replication